Slow Folding of a Three-Helix Protein via a Compact Intermediate†

Jia-Cherng Horng,‡,§ Sylvia M. Tracz,‡,§ Kevin J. Lumb,*,||,⊥ and Daniel P. Raleigh*,‡,@

Department of Chemistry, Graduate Program in Biophysics, and Graduate Program in Biochemistry and Structural Biology, State University of New York, Stony Brook, New York 11794-3400, and Department of Biochemistry and Molecular Biology, Colorado State University, Fort Collins, Colorado 80523-1870

Received June 3, 2004; Revised Manuscript Received October 11, 2004

ABSTRACT: The KIX domain of CREB binding protein (CBP) forms a small three-helix bundle which folds autonomously. Previous equilibrium unfolding experiments led to the suggestion that folding may not be strictly two-state. To investigate the folding mechanism in more detail, the folding kinetics of KIX have been studied by urea jump fluorescence-detected stopped-flow experiments. Clear evidence for an intermediate is obtained from the plot of the natural log of the observed rate constant versus denaturant concentration, the chevron plot, and from analysis of the initial fluorescence amplitudes of the stopped-flow experiments. The chevron plot exhibits a change in shape, rollover, at low denaturant concentrations, characteristic of the formation of an intermediate. The kinetic data can be fit to a three-state model involving a compact intermediate. An on-pathway model predicts that the position of the intermediate lies close to the native state. The folding rate in the absence of denaturant is 260 s^{-1} at pH 7.5 and 25 °C. This is significantly slower than the rates of other helical proteins similar in size. The slow folding may be due to the necessity of forming a buried polar interaction in the native state. The potential functional significance of the folding intermediate is discussed.

Determining how amino acid sequence encodes a given native state topology is a significant challenge for experimentalists and theoreticians studying protein folding. One approach to understanding protein folding is the identification and characterization of kinetic folding intermediates, which can provide insight into events during the folding process. Many proteins larger than 100 amino acids populate folding intermediates (*1*−*3*), while smaller proteins that lack disulfide bonds or proline isomerization often fold in a two-state fashion without populated intermediates (*4*, *5*). For a two-state folding protein, the folding rate is strongly related to topology or contact order (*6*, *7*). There is an excellent correlation between the log of the folding rate and native state topology as defined by contact order for proteins that fold in a two-state fashion. Small, all-helical, proteins with simple topologies have low contact order and are predicted to fold rapidly, and indeed, numerous small helical proteins have been shown to fold rapidly without forming intermediates (*8*, *9*).

The KIX domain of the transcriptional coactivator and histone acetyltransferase, CREB binding protein (CBP),[1] mediates interactions between CBP and various human and viral transcriptional activators (*10*−*12*). KIX is involved in numerous protein−protein complexes. Upon phosphorylation of CREB, KIX binds inducibly to CREB, and binds constitutively to a number of human and viral activators. CBP and the highly related protein p300 are both very large proteins of more than 2400 residues that contain several autonomously functional domains (*11*, *12*). One such domain is the 93-residue KIX domain (*13*). KIX contains three α-helices, two short 3_{10}-helices, and interconnecting loops that form a globular fold around a hydrophobic core (Figure 1). The three α-helices form a three-helix bundle with a simple up−down−up topology. KIX is monomeric, lacks disulfides, and does not require metal ions or bound cofactors to fold, and all of its prolines are in the trans configuration in the folded state (*13*−*16*). The small size, high helical content, and simple topology suggest that KIX should fold rapidly.

We have previously characterized the equilibrium unfolding of KIX (*14*). The equilibrium unfolding curves of KIX monitored with CD and fluorescence were not entirely equivalent (*14*). This observation suggests that KIX folding may not be strictly two-state. We also examined the role of a buried π−cation interaction involving Tyr 640 and Arg 600 in specifying a unique fold (*14*). The interaction is structurally important since disruption of the interaction by mutation of Arg 600 to Met resulted in a protein with the properties of a molten globule. In vitro, CARM1 methylates

† Supported by NIH Grant GM54233 (D.P.R.) and American Cancer Society Grant RSG-02-051-GMC (K.J.L.).

* To whom correspondence should be addressed. D.P.R.: phone, (631) 632-9547; fax, (631) 632-7960; e-mail, draleigh@notes.cc.sunysb.edu. K.J.L.: e-mail, kevin.lumb.b@bayer.com.

‡ Department of Chemistry, State University of New York.

§ These authors contributed equally to this work.

|| Colorado State University.

⊥ Present address: Bayer Pharmaceuticals Corp., 400 Morgan Lane, West Haven, CT 06516.

@ Graduate Program in Biophysics and Graduate Program in Biochemistry and Structural Biology, State University of New York.

[1] Abbreviations: $\Delta G_u°$, free energy of unfolding; ACBP, acyl-CoA-binding protein; CARM1, coactivator-associated arginine methyltransferase 1; CBP, CREB-binding protein; C_M, midpoint of the denaturant-induced unfolding transition; CREB, cyclic AMP response element binding protein; CD, circular dichroism; ANS, 1-anilinonaphthalene-8-sulfonate.

10.1021/bi048852p CCC: $30.25
Published on Web 12/22/2004

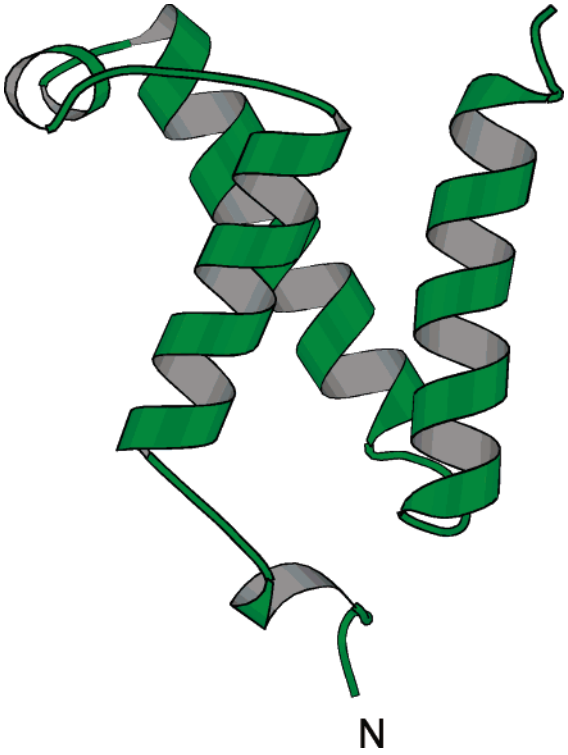

FIGURE 1: Structure of the KIX domain of CBP. The ribbon diagram was prepared using Molscript (*40*), and the KIX structure was from the KIX−pKID complex (Protein Data Bank entry 1KDX) (*13*).

Arg 600 of KIX (*14*, *17*). Methylation negatively regulates the binding of the KIX domain to CREB. Arg 600 is distant from the KIX−CREB binding interface, suggesting that a direct steric impediment to binding is unlikely. It is possible that methylation might modulate the Arg 600−Tyr 640 cation−π interaction.

Mutation of Arg 600 to Met led to a partially folded molten globule state that was rich in helical structure but lacked a cooperative thermal unfolding transition, had a tendency to aggregate, and bound the hydrophobic dye ANS (*14*). The formation of a molten globule-like state in the absence of the π−cation interaction suggests indirectly that intermediates might accumulate in the folding process. To directly address the potential role of intermediates during KIX folding, we have performed kinetic refolding studies using stopped-flow methods. Our results show that, despite the apparent structural simplicity and predicted fast folding rate, a compact kinetic folding intermediate is populated early during the refolding of KIX.

EXPERIMENTAL PROCEDURES

KIX Expression and Purification. KIX, corresponding to residues 587−679 of human CBP with an additional N-terminal Met, was expressed and purified as described previously (*15*, *18*). The identity and integrity of KIX were confirmed with electrospray mass spectrometry, and the expected and observed mass agreed to within 1 Da. The mouse CBP sequence numbering is used for ease of comparison with the majority of studies that use mouse CBP. The sequences of the human and mouse KIX domains of CBP are 100% identical over the folded region of KIX (*13*).

Equilibrium Unfolding. Urea denaturation experiments were performed as previously described (*14*). Measurements were conducted at 25 °C in 10 mM sodium phosphate and 150 mM NaCl (pH 7.5). Fluorescence studies were performed using a Spex Fluorolog spectrometer. The change in emission intensity at 355 nm was monitored following excitation at 276 nm. CD studies were conducted using an Aviv 202 spectrometer. The signal at 222 nm was monitored. The urea concentration was determined with refractometry. The protein concentration was approximately 4 μM, determined by absorbance using an excitation coefficient of 12 650 cm^{-1} M^{-1} at 276 nm. The free energy of unfolding and the *m* value were determined by nonlinear least-squares fitting of the complete unfolding curve assuming a monomer unfolding model. The pre- and post-transition baselines were modeled using linear functions of urea concentration.

Stopped-Flow Fluorescence. Stopped-flow fluorescence measurements were performed using an Applied Photophysics SX.18MV stopped-flow reaction analyzer equipped for asymmetric mixing at a ratio of 10:1. Fluorescence measurements were conducted with an excitation wavelength of 280 nm using a 320 nm cutoff filter. Experiments were performed at 25 °C on samples prepared in 10 mM sodium phosphate and 150 mM NaCl (pH 6.5 or 7.5). Final protein concentrations were approximately 45 μM unless otherwise noted. For refolding experiments, KIX was denatured in 6 M urea and folding was initiated by an 11-fold dilution into lower concentrations of urea. Unfolding experiments were initiated by an 11-fold dilution of KIX into higher concentrations of urea. The curves at each urea concentration were obtained by averaging three to five individual stopped-flow experiments.

The folding of KIX was fit to a three-state folding mechanism, with an obligate on-pathway intermediate (Scheme 1). The model assumes that formation of the intermediate is

Scheme 1

$$\mathrm{U} \underset{}{\overset{K_{UI}}{\rightleftharpoons}} \mathrm{I} \underset{k_{NI}}{\overset{k_{IN}}{\rightleftharpoons}} \mathrm{N}$$

a prerequisite for achieving the native state. Formation of the intermediate is assumed to be rapid, leading to a pre-equilibrium (defined by the equilibrium constant, K_{UI}), which occurs much faster than the rate-limiting step (k_{IN}) to the native state formation. Thus, the observed folding rate (k_f) can be defined by

$$k_f = f_I k_{IN} = [K_{UI}/(1 + K_{UI})]k_{IN} \quad (1)$$

where f_I is the fractional concentration of the intermediate. The plot of ln k_{obs} versus urea concentration was fit to eq 2 to determine the folding and unfolding rate constants in the absence of denaturant, k_{IN} and k_{NI}, respectively.

$$\ln k_{obs} = \ln\left[\frac{K_{UI}\exp(-m_{UI}[\mathrm{urea}]/RT)}{1 + K_{UI}\exp(-m_{UI}[\mathrm{urea}]/RT)}k_{IN} \times \exp(m_{IN}^{\neq}[\mathrm{urea}]/RT) + k_{NI}\exp(m_{NI}^{\neq}[\mathrm{urea}]/RT)\right] \quad (2)$$

where m_{UI}, $m_{IN}^{\neq}$, and $m_{NI}^{\neq}$ are constants that describe how the natural log of K_{UI}, k_{IN}, and k_{NI}, respectively, vary as a function of the concentration of urea. An off-pathway model was also examined in which the intermediate represents a

Scheme 2

$$\mathbf{I} \underset{}{\overset{K_{UI}}{\rightleftharpoons}} \mathbf{U} \underset{k_{NU}}{\overset{k_{UN}}{\rightleftharpoons}} \mathbf{N}$$

misfolded species (Scheme 2). In this scheme, the intermediate cannot fold directly to the native state but must unfold first to form U. The observed folding rate (k_f) is defined by

$$k_f = f_U k_{UN} = [K_{IU}/(1 + K_{IU})]k_{UN} = [1/(1 + K_{UI})]k_{UN} \quad (3)$$

where f_U is the fractional concentration of the unfolded state. Using this model, the chevron plot of ln k_{obs} versus urea concentration was fit to the following equation to determine the folding and unfolding rate constants in the absence of denaturant, k_{UN} and k_{NU}, respectively.

$$\ln k_{obs} = \ln\left[\frac{1}{1 + K_{UI}\exp(-m_{UI}[\text{urea}]/RT)}k_{UN} \times \exp(m_{UN}^{\neq}[\text{urea}]/RT) + k_{NU}\exp(m_{NU}^{\neq}[\text{urea}]/RT)\right] \quad (4)$$

where m_{UI}, $m_{UN}^{\neq}$, and $m_{NU}^{\neq}$ are constants that describe how the natural log of K_{UI}, k_{UN}, and k_{NU}, respectively, vary as a function of the concentration of urea.

RESULTS

KIX contains a single buried Trp residue at position 591 in the first 3_{10}-helix (*13*). This residue is largely buried in the hydrophobic core. The fluorescence emission undergoes a significant shift in maximum from 307 to 355 nm and an increase in quantum yield upon unfolding and thus provides a convenient probe for folding studies (*14*).

The stability of KIX is pH-dependent with the domain becoming more thermostable as the pH is increased from 4 to 7.5 (*18*). The stability, as measured with urea denaturation, increases from pH 4 to 7.5 but is the same at pH 7.5 and 8.5 (data not shown). Experiments were performed at pH 7.5 so that the folding kinetics would be determined under conditions where the native state appears to be more stable. A similar set of measurements was also performed at pH 6.0, to match conditions used in our initial equilibrium unfolding studies of the domain (*14*).

Non-Two-State Folding. The CD and fluorescence-monitored urea-induced equilibrium unfolding curves show a slight deviation from exact overlap at pH 7.5 (Figure 2) similar to that observed previously at pH 6.0 (*14*). The fluorescence-monitored unfolding curve is steeper. This suggests that folding might not be strictly two-state. Fitting the CD-monitored curve to an apparent two-state transition yields an apparent midpoint, C_M, of 3.62 M urea, an apparent m value of 0.96 kcal mol^{-1} M^{-1}, and an extrapolated apparent stability in H_2O of -3.48 kcal/mol. Analysis of the fluorescence-detected unfolding data yields an apparent C_M value of 3.48 M urea, an apparent m value of 1.18 kcal mol^{-1} M^{-1}, and an extrapolated apparent stability in H_2O of -4.1 kcal/mol.

Kinetic folding and unfolding experiments were conducted by urea jump stopped-flow fluorescence detection. The individual stopped-flow traces exhibited a major fast phase consisting of approximately 90% of the amplitude and a slow phase accounting for the remaining 10% with a time constant of 100 s that is consistent with proline isomerism. The dead time of the instrument is on the order of 3.5 ms; thus, very rapid phases would not be directly detectable in a single curve. The major phase could be fit well by a single exponential at all final urea concentrations. Representative refolding and unfolding traces are shown in Figure 3.

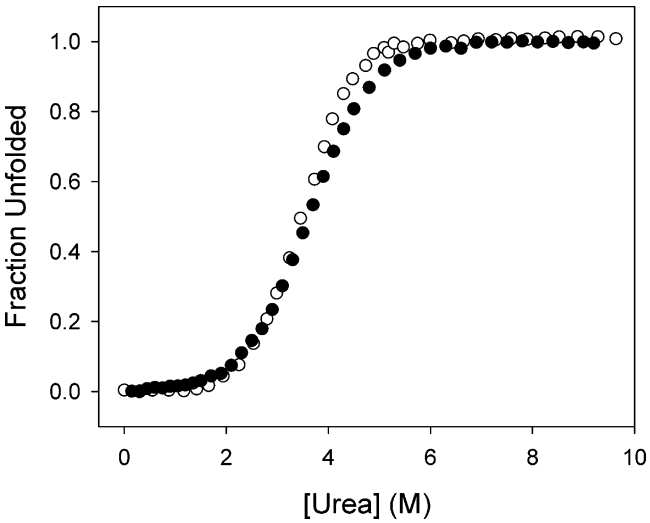

FIGURE 2: Equilibrium unfolding curves for the urea denaturation of KIX at pH 7.5 and 25 °C, 10 mM sodium phosphate, 150 mM NaCl. Curves are displayed as plots of the fraction unfolded measured with fluorescence (○) or the CD signal at 222 nm (●).

The chevron plot allows detection of unresolved intermediates (*19*). In the case of two-state folding, both branches of the chevron plot are expected to be linear (*19*). In contrast, the population of a rapidly formed intermediate leads to a change in slope at low denaturant concentrations (rollover). The chevron plot for KIX clearly deviates from the V shape expected for simple two-state folding (Figure 4). Transient aggregation during refolding can lead to rollover in chevron plots (*20*). Consequently, we examined the concentration dependence of the refolding rate in the rollover region. Refolding rates at 0.55 M urea were measured for samples ranging from a final protein concentration of 5 to 100 μM (Figure 5). The same rate was observed at all protein concentrations that were tested (5, 45, and 100 μM), arguing against transient aggregation. Deviations from linear chevron plots can also arise from transition state movement. This often results in symmetrically curved chevrons. The unfolding branch of the KIX chevron appears to be linear, suggesting that transition state movement is not occurring.

Additional evidence for non-two-state folding comes from the analysis of the fluorescence amplitudes of the stopped-flow experiment (burst phase analysis) (*1*, *21*). Figure 6 shows a plot of the final and extrapolated initial fluorescence intensity of the stopped-flow measurements as a function of urea concentration. The final signals correspond to the equilibrium signal at a given urea concentration, while the initial signals are the values extrapolated to time zero using the observed experimental curves at a given urea concentration. For simple two-state folding, the initial signals for refolding experiments will lie on the post-transition line, which indicates that the initial signals are purely due to the unfolded state (*1*, *21*). In contrast, the initial fluorescence signals of the refolding curves for KIX significantly deviate from the post-transition line, suggesting that the folding is multistate and kinetic folding intermediates exist.

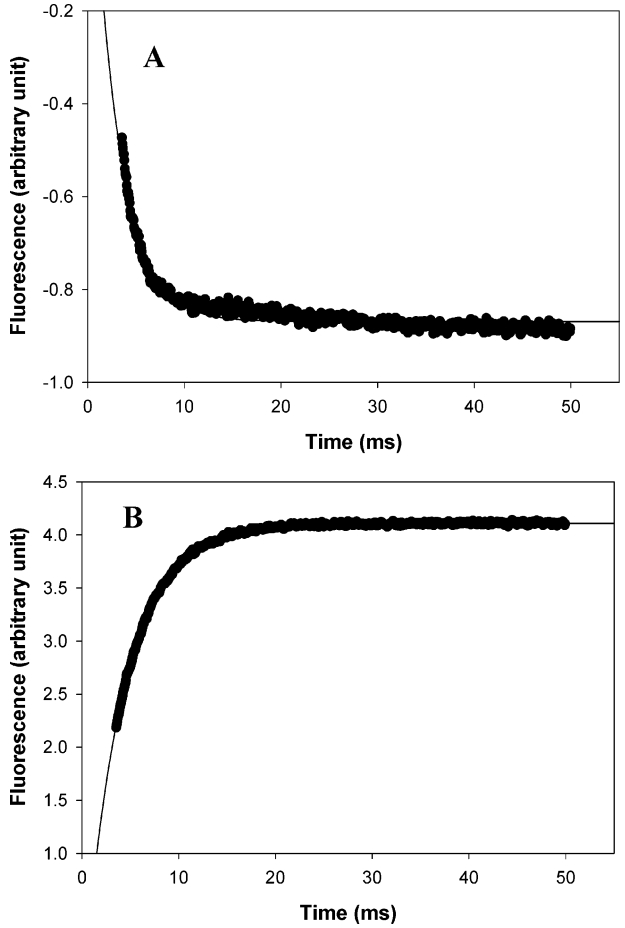

FIGURE 3: Stopped-flow traces for the refolding and unfolding of KIX at pH 7.5 and 25 °C. (A) Refolding curve at a final urea concentration of 1.6 M. (B) Unfolding curve collected at a final urea concentration of 8.5 M. Solutions contained 150 mM NaCl and were buffered using 10 mM phosphate.

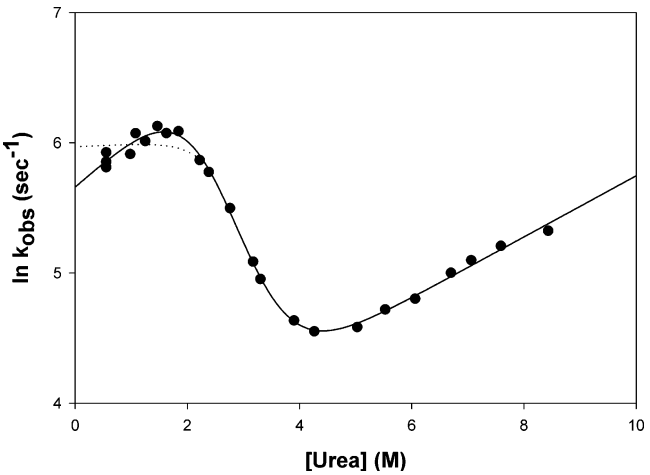

FIGURE 4: Plot of ln k_{obs} vs the concentration of urea for the folding and unfolding of KIX at pH 7.5 and 25 °C, 10 mM sodium phosphate, 150 mM NaCl. The lines indicate the best fit to the three-state on-pathway model described in Experimental Procedures. The solid line is the unconstrained fit, while the dotted line is from the fit with $m_{IN}^{\neq}$ constrained to be ≤ 0.

The final signals effectively trace out the equilibrium unfolding transition. A fit of the curve generated by these points to the standard expression for two-state folding gives an apparent midpoint, C_M, of 3.4 M which is in excellent agreement with the equilibrium value of 3.48 M (Figure 2).

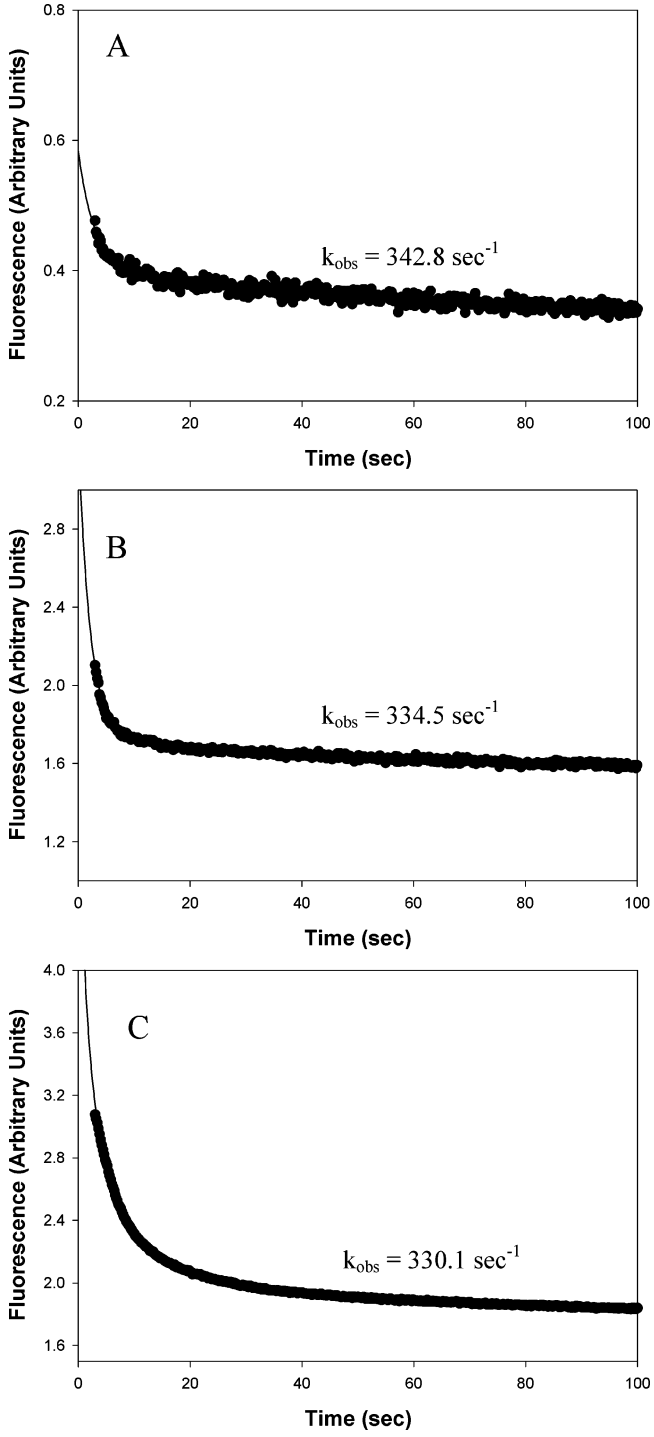

FIGURE 5: Stopped-flow traces for the refolding of KIX collected as a function of final protein concentrations. All experiments were conducted at a final urea concentration of 0.55 M: (A) 5 μM KIX, (B) 45 μM KIX, and (C) 100 μM KIX. The respective rate constants are shown. Experiments were conducted at pH 7.5 and 25 °C in 150 mM NaCl and 10 mM phosphate.

The apparent stability is −3.7 kcal/mol. This value corresponds to the 90% of the population represented by the major phase and needs to be corrected for cis−trans proline isomerism in the unfolded state (22). The corrected value, −3.6 kcal/mol, is in reasonable agreement with the apparent equilibrium value of −4.1 kcal/mol obtained by fitting the equilibrium fluorescence unfolding data. The plot of the initial signals as a function of urea concentration can be viewed as an unfolding curve for the intermediate. As expected, the

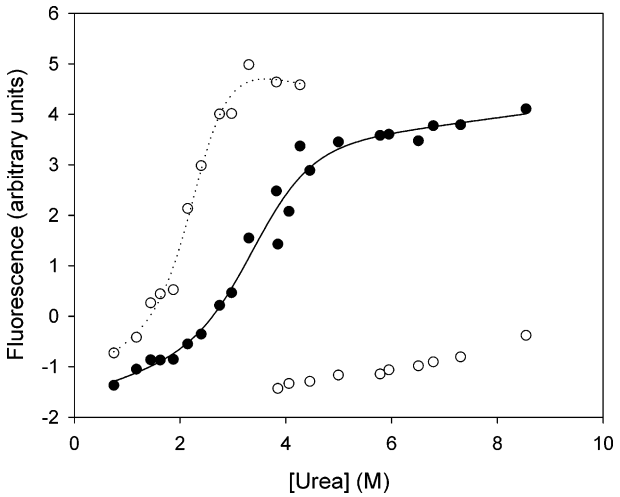

FIGURE 6: Plot of final (●) and initial fluorescence (○) intensities from kinetic experiments vs urea concentration for KIX at pH 7.5 and 25 °C, 10 mM sodium phosphate, 150 mM NaCl. The fluorescence signals were derived from stopped-flow experiments. The final signals are similar to the signal from an equilibrium unfolding curve, and the empty circles can be regarded as an unfolding curve for the intermediate. The solid lines indicate the fit for a two-state model using standard methods.

intermediate is less stable with an apparent C_M of 2.3 M urea. The stability of the intermediate can be estimated using the C_M value and the *m* value. Directly fitting the initial amplitude to the expression for equilibrium two-state folding provides an estimated *m* value (1.8 ± 1.0 kcal mol^{-1} M^{-1}), but it is not very reliable because there are only a few points in the pretransition region and the post-transition has a significant slope. Analysis of the kinetic data described below provides an estimated *m* value for the U to I transition (1.33, Table 1). Using this value leads to an apparent stability on the order of 3.1 kcal/mol. A similar value is obtained if the *m* value for the complete equilibrium N to U transition is used.

Kinetic experiments were also performed at pH 6.0. The signal to noise ratio of the measurements is not as good under these conditions, but the rollover in the chevron plot is clearly visible. Analysis of the initial and final amplitudes of the experiments carried out at pH 6 shows the presence of a burst phase under these conditions. The intermediate appears to be less stable at pH 6.0 with the apparent C_M slightly reduced to 1.7 M urea. Thus, the decreased native state stability at pH 6.0 relative to that at pH 7.5 is mirrored by a decrease in the stability of the intermediate.

Folding Pathway Analysis of Kinetic Data. The kinetic data can be modeled in terms of a linear three-state process involving an on-pathway intermediate. The I to U transition is rapid and cannot be directly observed. For Scheme 1, the kinetic analysis yields values for rate constants k_{IN} and k_{NI} and the apparent equilibrium constant K_{UI} (Table 1). Fitting the data to the on-pathway model gives a K_{UI} of 149, a k_{IN} of 259 s^{-1}, and a k_{NI} of 29.9 s^{-1}.

A model involving a nonproductive off-pathway intermediate also fit the data. For Scheme 2, the kinetic analysis yields values for rate constants k_{UN} and k_{NU} and the apparent equilibrium constant K_{UI} (Table 1). The analysis leads to values for K_{UI} of 149 s^{-1}, k_{UN} of 38 500 s^{-1}, and k_{NU} of 29.9 s^{-1}. It is formally impossible to distinguish the on-pathway from the off-pathway model with the kinetic data at hand. The off-pathway model seems to be less physical since it involves folding to an intermediate which is almost as compact as the native state. This intermediate is then required to completely unfold to reach the native state in the off-pathway scenario. In addition, the model yields a folding rate on the order of 40 000 s^{-1}, which is almost 1 order of magnitude larger than the value obtained by linear extrapolation of the chevron plot over the region where there is no rollover.

m values for a transition reflect the change in solvent accessible surface area between the two states. The fit to the on-pathway model (Scheme 1) yields values for $m_{IN}^{\neq}$, $m_{NI}^{\neq}$, and m_{UI}. The $m_{IN}^{\neq}$ value describes the dependence of ln k_{IN} on urea concentration, while m_{UI} is related to the urea dependence of ln K_{UI} and $m_{NI}^{\neq}$ to the dependence of ln k_{NI} on urea concentration. $m_{IN}^{\neq}$ is relatively small, indicating that k_{IN} is weakly dependent on urea concentration. An unconstrained fit gives a positive value of $m_{IN}^{\neq}$ (0.24 ± 0.04 kcal mol^{-1} M^{-1}). $m_{IN}^{\neq}$ is related to the change in buried surface area between I and the transition state for folding. Normally, $m_{IN}^{\neq}$, or $m_f^{\neq}$ for a two-state folder, is expected to be less than zero because the transition state is more compact than the starting state. It is difficult to rationalize the apparent positive slope since it formally suggests that the transition state is less compact then I. One possibility is that such an effect might arise if the intermediate needs to partially unfold to form the rate-limiting transition state. The slope of the chevron plot at low urea concentrations is small and determined by relatively few points that exhibit some scatter (Figure 4). The data can also be well fit by a model which constrains $m_{IN}^{\neq}$ to be less than or equal to zero. The rate constants obtained with this are k_{IN} (355 ± 31 s^{-1}) and k_{NI} (36 ± 6.2 s^{-1}) and are in good agreement with those obtained from the unconstrained fit (Table 1). The value of the pre-equilibrium constant is larger, but the uncertainty is great (K_{UI} is equal to 2900 ± 5100 s^{-1}).

Comparison of Kinetic Refolding and Equilibrium Unfolding Data. The apparent stability and *m* mvalues determined from fluorescence-monitored equilibrium unfolding experiments can be compared to the values calculated from the rate constants as a test of internal consistency. The kinetic analysis is concerned with only the major phase, and thus, the values need to be corrected for the effects of cis−trans isomerism in the unfolded state. The uncorrected $\Delta G°$ value is given by

$$\Delta G° = -RT \ln(K_{UI} k_{IN}/k_{NI}) \quad (5)$$

and the *m* value is given by

$$m_{UN} = m_{UI} + m_{NI}^{\neq} - m_{IN}^{\neq} \quad (6)$$

The corrected value of $\Delta G°$ is −4.2 kcal/mol. This is in good agreement with the apparent $\Delta G°$ value (−4.1 kcal/mol) determined from equilibrium fluorescence measurements. The calculated *m* value is 1.24 kcal mol^{-1} M^{-1}, while the equilibrium value from fluorescence is 1.2 kcal mol^{-1} M^{-1}. The differences are small and are less than deviations that have been reported for other three-state folding proteins (*23*). The deviation from the apparent equilibrium parameters

Table 1: Kinetic Parameters for the Folding of KIX at pH 7.5 and 25 °C Derived from Fits to (A) an Unconstrained On-Pathway Model, (B) a Constrained On-Pathway Model in Which $m_{IN}^{\neq} \leq 0$, and (C) an Off-Pathway Model[a]

(A) Unconstrained On-Pathway Model

K_{UI} (s^{-1})	m_{UI} (kcal mol^{-1} M^{-1})	k_{IN} (s^{-1})	k_{NI} (s^{-1})	$m_{IN}^{\neq}$ (kcal mol^{-1} M^{-1})	$m_{NI}^{\neq}$ (kcal mol^{-1} M^{-1})
149 ± 65	1.33 ± 0.06	259 ± 14	29.9 ± 3.1	0.24 ± 0.04	0.14 ± 0.01

(B) Constrained On-Pathway Model ($m_{IN}^{\neq} \leq 0$)

K_{UI} (s^{-1})	m_{UI} (kcal mol^{-1} M^{-1})	k_{IN} (s^{-1})	k_{NI} (s^{-1})	$m_{IN}^{\neq}$ (kcal mol^{-1} M^{-1})	$m_{NI}^{\neq}$ (kcal mol^{-1} M^{-1})
2897 ± 5148	1.68 ± 0.31	355 ± 31	36 ± 6.2	≤0	0.12 ± 0.02

(C) Unconstrained Off-Pathway Model

K_{UI} (s^{-1})	m_{UI} (kcal mol^{-1} M^{-1})	k_{UN} (s^{-1})	k_{NU} (s^{-1})	$m_{UN}^{\neq}$ (kcal mol^{-1} M^{-1})	$m_{NU}^{\neq}$ (kcal mol^{-1} M^{-1})
149 ± 66	1.33 ± 0.06	38500 ± 17900	29.9 ± 3.1	−1.1 ± 0.09	0.14 ± 0.009

[a] Experiments were conducted in 10 mM phosphate and 150 mM NaCl buffer.

deduced by analysis of the CD data ($\Delta G° = -3.5$ kcal/mol, $m = 0.96$ kcal mol^{-1} M^{-1}) is somewhat larger.

DISCUSSION

Previous equilibrium unfolding studies with CD and fluorescence spectroscopy of the KIX domain of CBP at pH 6.0 led to the suggestion that folding might not be strictly two-state. The difference between the experimental unfolding curves measured with the two techniques was, however, less than is often observed for proteins that do not follow two-state folding (*14*). The kinetic analysis presented here shows clearly that folding is not two-state. Modeling the folding process with a three-state on-pathway model indicates that the protein rapidly forms a compact intermediate and then subsequently folds to the native state at a rate on the order of 260 s^{-1}. The rate is slow compared to those of several other well-characterized helical proteins (*9*). For example, an 80-residue monomeric variant of λ-repressor, the 60-residue B-domain of protein A, and the 73-residue designed protein α-3D fold on the microsecond time scale (*24*−*29*). The 86-residue Im9 protein folds with a rate of 1450 s^{-1}, while the extrapolated rate for cytochrome c_{553} is 5300 s^{-1} (*23*, *30*). The folding rate of KIX is also slower than those of several other all helical proteins that form intermediates. These include ACBP, the FF domain, and the engrailed homeodomain, which exhibit folding rates ranging from 650 to more than 30 000 s^{-1} (*23*, *31*−*33*).

Early arguments suggested that intermediates would be less likely to be observed in small relatively unstable proteins (*4*). However, this is not the case for KIX. KIX is only modestly stable with a $\Delta G°$ of 3.5−4.1 kcal/mol, and still forms an intermediate. Two other small, modestly stable, helical proteins have recently been shown to populate folding intermediates. Both the helical FF domain and the immunity protein Im7 have fewer than 100 residues and are not particularly stable yet form intermediates (*23*, *31*). It is apparent, therefore, that the ability to form a populated folding intermediate is dependent on the details of the sequence rather than on the global stability or size.

The observed folding rate of KIX is significantly lower than that predicted by its relative contact order or by the topomer search model of two-state folding (*6*, *7*, *34*). The relative contact order of KIX is 9%, calculated using the NMR structure, which leads to a predicted folding rate of 3.6×10^4 s^{-1}. The topomer search model predicts a rate of 2×10^4 s^{-1} (*34*). It has been suggested that the accumulation of folding intermediates may slow the rate of folding relative to that expected for a two-state mechanism (*35*−*37*). The slow observed rate constant for KIX suggests that this could be the case here. Note, however, that folding intermediates do not always have to lead to slower folding (*38*, *39*).

The slow folding rate of KIX is striking given the simple nature of the protein, which is monomeric and helical and lacks disulfide bonds or cofactors. One structural feature of KIX which is important for the acquisition of native structure is a buried polar interaction involving Tyr 640 and Arg 600 (*13*). It is possible that the formation of this buried polar interaction which involves desolvation of a charged side chain contributes to slow folding. The formation of a buried polar interaction has been shown to slow folding in other systems. For example, replacement of a buried salt bridge triad of the Arc repressor results in a significantly faster folding (*40*).

The KIX folding intermediate is quite compact based on the urea dependence of the kinetic parameters. The Tanford β-parameter or β_I, which is the ratio of the *m* value for the U to I transition to the *m* value for complete folding, U to N, is commonly used as a measure of the compactness of an intermediate. Reported β_I values range from a low of 0.34 for ACBP to a high of 0.93 for the immunity protein Im9 at low pH, with all values of β_I greater than 0.7 except for those of ACBP and Rnase H (*23*, *31*, *32*, *41*, *42*). The value is close to 1 for KIX, suggesting that I is compact and much closer to the native state than to the unfolded state. There is a precedent for compact intermediates from studies of other proteins (*23*, *31*, *41*). It is tempting but difficult to speculate about the nature of the I to N transition. The transition occurs between two compact states and thus might involve relatively subtle structural rearrangements, perhaps involving the cation−π interaction. Breaking this interaction via mutation of Arg 600 to Met has been shown to lead to a compact molten globule-like stucture. Other possibilities include exclusion of water from a partially desolvated core (*43*), or perhaps disruption of interactions that need to be broken to form the rate-limiting transition state.

The lifetime of the native state of the KIX domain is relatively short with a rate of unfolding from N to I of ∼30 s^{-1}. KIX functions as a protein recognition domain and mediates a number of important protein−protein interactions. The ability of KIX to bind the transcriptional activator CREB is negatively regulated by methylation by CARM1 of KIX at Arg 600 (*44*). Arg 600 is both buried and critical for the

formation of the native fold (*14*). It is intriguing to speculate that the relatively rapid unfolding of KIX might play a functional role in the regulation of KIX by rendering Arg 600 susceptible to methylation.

We conclude that KIX folds relatively slowly via a compact intermediate. This behavior is striking given the structural simplicity of KIX. The presence of the compact intermediate leads to a view of KIX folding that is more aligned with a folding pathway that proceeds via collapse to a compact intermediate that is followed by reorganization to the native structure as opposed to a rapid diffusion−collision mechanism.

ACKNOWLEDGMENT

We thank K. M. Campbell and Y. Wei for purified KIX, J. Cho for assistance with kinetic measurements, and Prof. K. W. Plaxco for performing the topomer search calculations.

SUPPORTING INFORMATION AVAILABLE

A chevron plot and a plot of initial and final amplitudes for the folding of KIX at pH 6.0. This material is available free of charge via the Internet at http://pubs.acs.org.

REFERENCES

1. Roder, H., and Colon, W. (1997) Kinetic role of early intermediates in protein folding, *Curr. Opin. Strut. Biol. 7*, 15−28.
2. Sanchez, I. E., and Kiefhaber, T. (2003) Evidence for sequential barriers and obligatory intermediates in apparent two-state protein folding, *J. Mol. Biol. 325*, 367−376.
3. Matthews, C. R. (1993) Pathways of protein folding, *Annu. Rev. Biochem. 62*, 653−683.
4. Jackson, S. E. (1998) How do small single-domain proteins fold? *Folding Des. 3*, R81−R91.
5. Kamagata, K., Arai, M., and Kuwajima, K. (2004) Unification of the folding mechanisms of non-two-state and two-state proteins, *J. Mol. Biol. 339*, 951−965.
6. Plaxco, K. W., Simons, K. T., Ruczinski, I., and Baker, D. (2000) Topology, stability, sequence, and length: Defining the determinants of two-state protein folding kinetics, *Biochemistry 39*, 11177−11183.
7. Plaxco, K. W., Simons, K. T., and Baker, D. (1998) Contact order, transition state placement and the refolding rates of single domain proteins, *J. Mol. Biol. 277*, 985−994.
8. Myers, J. K., and Oas, T. G. (2002) Mechanism of fast protein folding, *Annu. Rev. Biochem. 71*, 783−815.
9. Kubelka, J., Hofrichter, J., and Eaton, W. A. (2004) The protein folding "speed limit", *Curr. Opin. Strut. Biol. 14*, 76−88.
10. Vendel, A. C., and Lumb, K. J. (2003) Molecular recognition of the human coactivator CBP by the HIV-1 transcriptional activator Tat, *Biochemistry 42*, 910−916.
11. Chan, H. M., and La Thangue, N. B. (2001) p300/CBP proteins: HATs for transcriptional bridges and scaffolds, *J. Cell Sci. 114*, 2363−2373.
12. Goodman, R. H., and Smolik, S. (2000) CBP/p300 in cell growth, transformation, and development, *Genes Dev. 14*, 1553−1577.
13. Radhakrishnan, I., Perez-Alvarado, G. C., Parker, D., Dyson, H. J., Montminy, M. R., and Wright, P. E. (1997) Solution structure of the KIX domain of CBP bound to the transactivation domain of CREB: A model for activator: Coactivator interactions, *Cell 91*, 741−752.
14. Wei, Y., Horng, J. C., Vendel, A. C., Raleigh, D. P., and Lumb, K. J. (2003) Contribution to stability and folding of a buried polar residue at the CARM1 methylation site of the KIX domain of CBP, *Biochemistry 42*, 7044−7049.
15. Campbell, K. M., and Lumb, K. J. (2002) Structurally distinct modes of recognition of the KIX domain of CBP by Jun and CREB, *Biochemistry 41*, 13956−13964.
16. Radhakrishnan, I., Perez-Alvarado, G., Parker, D., Dyson, H. J., Montimony, M., and Wright, P. (1999) Structural analyses of CREB-CBP transcriptional activator-complexes by NMR spectroscopy: Implications for mapping the boundries of structural domains, *J. Mol. Biol. 287*, 859−865.
17. Xu, W., Chen, H., Du, K., Asahara, H., Tini, M., Emerson, B. M., Montminy, M., and Evans, R. M. (2001) A transcriptional switch mediated by cofactor methylation, *Science 294*, 2507−2511.
18. Mestas, S. P., and Lumb, K. J. (1999) Electrostatic contribution of phosphorylation to the stability of the CREB-CBP activator-coactivator complex, *Nat. Struct. Biol. 6*, 613−614.
19. Baldwin, R. L. (1996) On-pathway versus off-pathway folding intermediates, *Folding Des. 1*, R1−R8.
20. Oliveberg, M. (1998) Alternative explanations for "multistate" kinetics in protein folding: Transient aggregation and changing transition-state ensembles, *Acc. Chem. Res. 31*, 765−772.
21. Khorasanizadeh, S., Peters, I. D., and Roder, H. (1996) Evidence for a three-state model of protein folding from kinetic analysis of ubiquitin variants with altered core residues, *Nat. Struct. Biol. 3*, 193−205.
22. Jackson, S. E., and Fersht, A. R. (1991) Folding of chymotrpsin inhibitor 2. 1. Evidence for a two-state transition, *Biochemistry 30*, 10428−10435.
23. Ferguson, N., Capaldi, A. P., James, R., Kleanthous, C., and Radford, S. E. (1999) Rapid folding with and without populated intermediates in the homologous four-helix proteins Im7 and Im9, *J. Mol. Biol. 286*, 1597−1608.
24. Burton, R. E., Huang, G. S., Daugherty, M. A., Calderone, T. L., and Oas, T. G. (1997) The energy landscape of a fast-folding protein mapped by Ala-Gly substitution, *Nat. Struct. Biol. 4*, 305−310.
25. Vu, D. M., Myers, J. K., Oas, T. G., and Dyer, R. B. (2004) Probing the folding and unfolding dynamics of secondary and tertiary structures in a three-helix bundle protein, *Biochemistry 43*, 3582−3589.
26. Huang, G. S., and Oas, T. G. (1995) Submillisecond folding of monomeric λ repressor, *Proc. Natl. Acad. Sci. U.S.A. 92*, 6878−6882.
27. Myers, J. K., and Oas, T. G. (2001) Preorganized secondary structure as an important determinant of fast protein folding, *Nat. Struct. Biol. 8*, 552−558.
28. Sato, S., Religa, T. L., Daggett, V., and Fersht, A. R. (2004) Testing protein-folding simulations by experiment: B domain of protein A, *Proc. Natl. Acad. Sci. U.S.A. 101*, 6952−6956.
29. Zhu, Y., Alonso, D. O. V., Maki, K., Huang, C. Y., Lahr, S. J., Daggett, V., Roder, H., DeGrado, W. F., and Gai, F. (2003) Ultrafast folding of α_3D: A *de novo* designed three-helix bundle protein, *Proc. Natl. Acad. Sci. U.S.A. 100*, 15486−15491.
30. Guidry, J., and Wittung-Stafshede, P. (2000) Cytochrome c_{553}, a small heme protein that lacks misligation in its unfolded state, folds with rapid two-state kinetics, *J. Mol. Biol. 301*, 769−773.
31. Jemth, P., Gianni, S., Day, R., Li, B., Johnson, C. M., Daggett, V., and Fersht, A. R. (2004) Demonstration of a low-energy on-pathway intermediate in a fast-folding protein by kinetics, protein engineering, and simulation, *Proc. Natl. Acad. Sci. U.S.A. 101*, 6450−6455.
32. Teilum, K., Maki, K., Kragelund, B. B., Poulsen, F. M., and Roder, H. (2002) Early kinetic intermediate in the folding of acyl-CoA binding protein detected by fluorescence labeling and ultrarapid mixing, *Proc. Natl. Acad. Sci. U.S.A. 99*, 9807−9812.
33. Mayor, U., Johnson, C. M., Daggett, V., and Fersht, A. R. (2000) Protein folding and unfolding in microseconds to nanoseconds by experiment and simulation, *Proc. Natl. Acad. Sci. U.S.A. 97*, 13518−13522.
34. Makarov, D., and Plaxco, K. (2003) The topomer search model: A simple, quantitative theory of two-state protein folding kinetics, *Protein Sci. 12*, 17−26.
35. Creighton, T. E. (1994) The energetic ups and downs of protein folding, *Nat. Struct. Biol. 1*, 135−138.
36. Fersht, A. R. (1995) Optimization of rates of protein folding: The nucleation-condensation mechasnism and its implications, *Proc. Natl. Acad. Sci. U.S.A. 92*, 10869−10873.
37. Sosnick, T. R., Mayne, L., Hiller, R., and Englander, S. W. (1994) The barriers in protein folding, *Nat. Struct. Biol. 1*, 149−156.
38. Calloni, G., Taddei, N., Plaxco, K. W., Ramponi, G., Stefani, M., and Chiti, F. (2003) Comparison of the folding processes of distantly related proteins. Importance of hydrophobic content in folding, *J. Mol. Biol. 330*, 577−591.
39. Wagner, C., and Kiefhaber, T. (1999) Intermediates can accelerate protein folding, *Proc. Natl. Acad. Sci. U.S.A. 96*, 6716−6721.

40. Waldburger, C. D., Jonsson, T., and Sauer, R. T. (1996) Barriers to protein folding: Formation of buried polar interactions is a slow step in acquisition of structure, *Proc. Natl. Acad. Sci. U.S.A. 93*, 2629−2634.
41. Gorski, S. A., Capaldi, A. P., Kleanthous, C., and Radford, S. E. (2001) Acidic condition stabilise intermediates populated during the folding of Im7 and Im9, *J. Mol. Biol. 312*, 849−863.
42. Spudich, G. M., Miller, E. J., and Marqusee, S. (2004) Destabilization of the *Escherichia coli* RNase H kinetic intermediate: Switching between a two-state and three-state folding mechanism, *J. Mol. Biol. 335*, 609−618.
43. Cheung, M., Garcia, A., and Onuchic, J. (2002) Protein folding mediated by solvation: Water expulsion and formation of the hydrophobic core occur after the structural collapse, *Proc. Natl. Acad. Sci. U.S.A. 99*, 685−690.
44. Kraulis, P. J. (1991) MOLSCRIPT: A program to produce both detailed and schematic plots of protein structures, *J. Appl. Crystallogr. 24*, 946−950.

BI048852P